

1    *Supplementary information*

2    **Rapid transition in winter aerosol composition in Beijing from  
3    2014 to 2017: response to clean air actions**

4    Haiyan Li<sup>1,a</sup>, Jing Cheng<sup>2</sup>, Qiang Zhang<sup>2</sup>, Bo Zheng<sup>3</sup>, Yuxuan Zhang<sup>2</sup>, Guangjie Zheng<sup>1</sup>, Kebin  
5    He<sup>1,3</sup>

6    <sup>1</sup> State Key Joint Laboratory of Environment Simulation and Pollution Control, School of Environment, Tsinghua  
7    University, Beijing 100084, China

8    <sup>2</sup> Ministry of Education Key Laboratory for Earth System Modeling, Department of Earth System Science, Tsinghua  
9    University, Beijing 100084, China

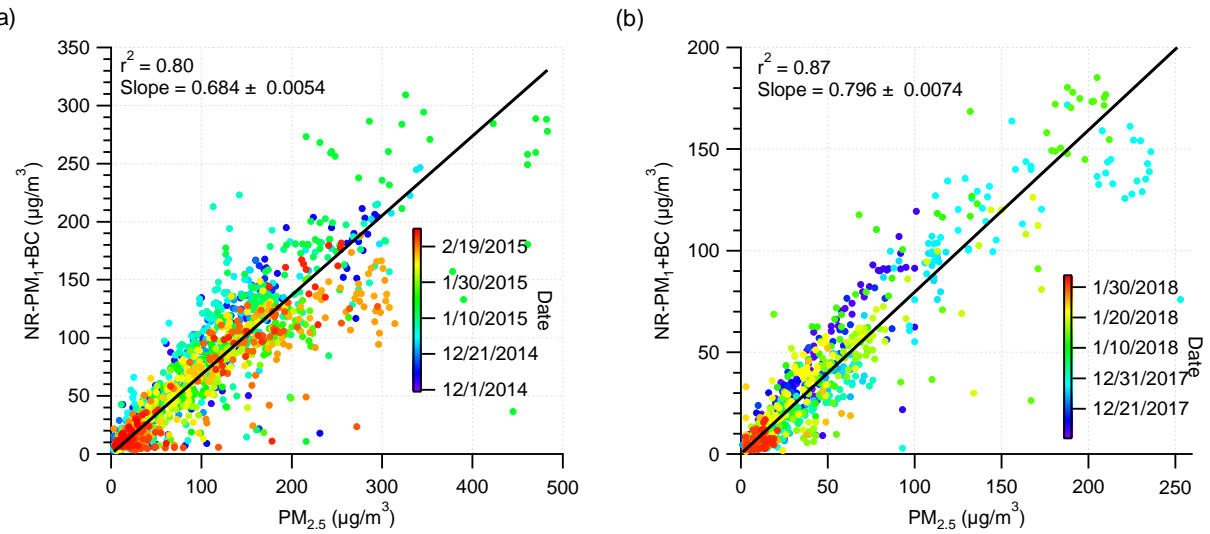
10    <sup>3</sup> State Environmental Protection Key Laboratory of Sources and Control of Air Pollution Complex, Tsinghua  
11    University, Beijing 100084, China

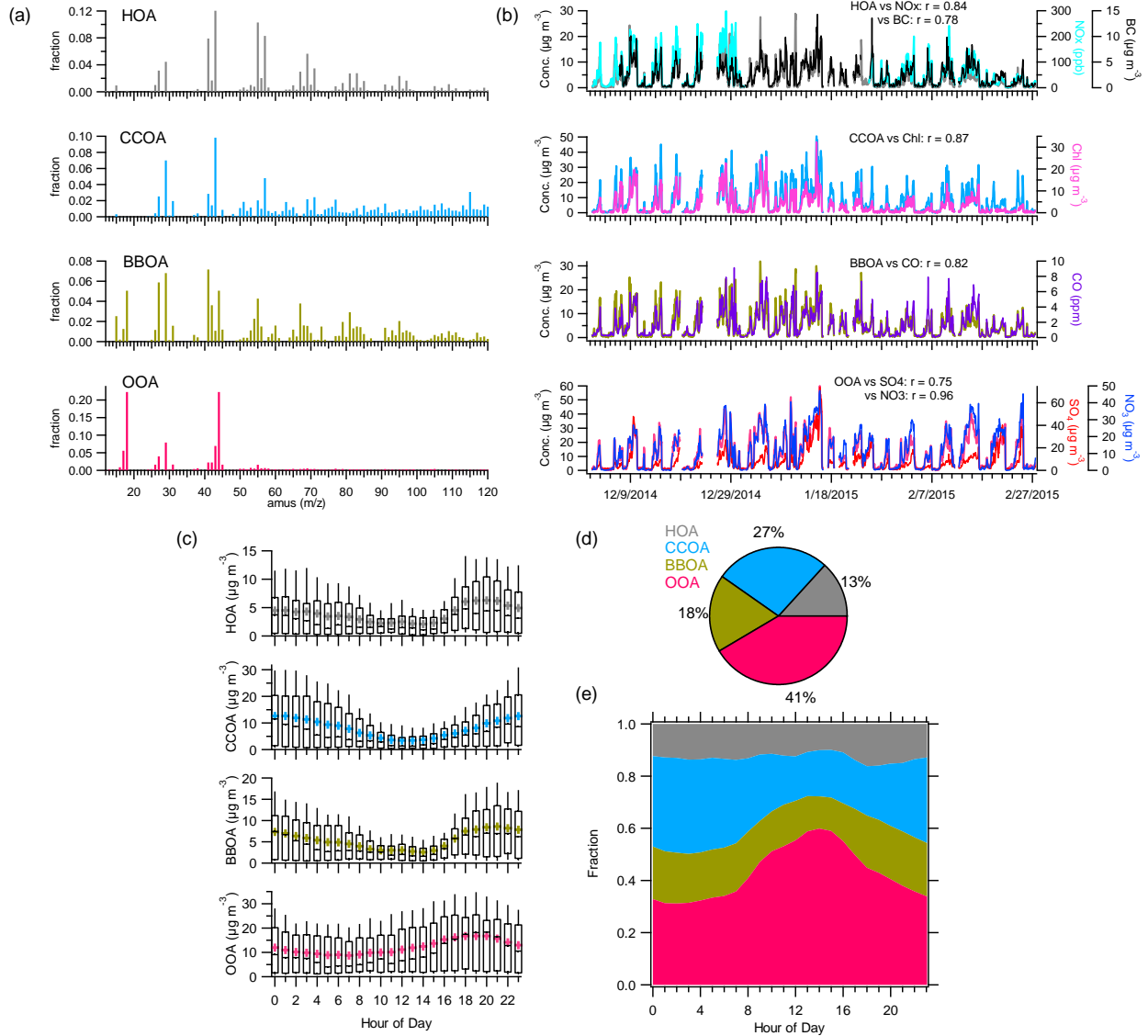
12    <sup>a</sup>present address: Institute for Atmospheric and Earth System Research/Physics, Faculty of Science, University of  
13    Helsinki, 00014 Helsinki, Finland

14    Correspondence: Qiang Zhang ([qiangzhang@tsinghua.edu.cn](mailto:qiangzhang@tsinghua.edu.cn))

15

16 **Figure S1.** Correlation of total PM<sub>1</sub> concentration (NR-PM<sub>1</sub> plus BC) with PM<sub>2.5</sub> concentration  
17 during the winter of (a) 2014 and (b) 2017.

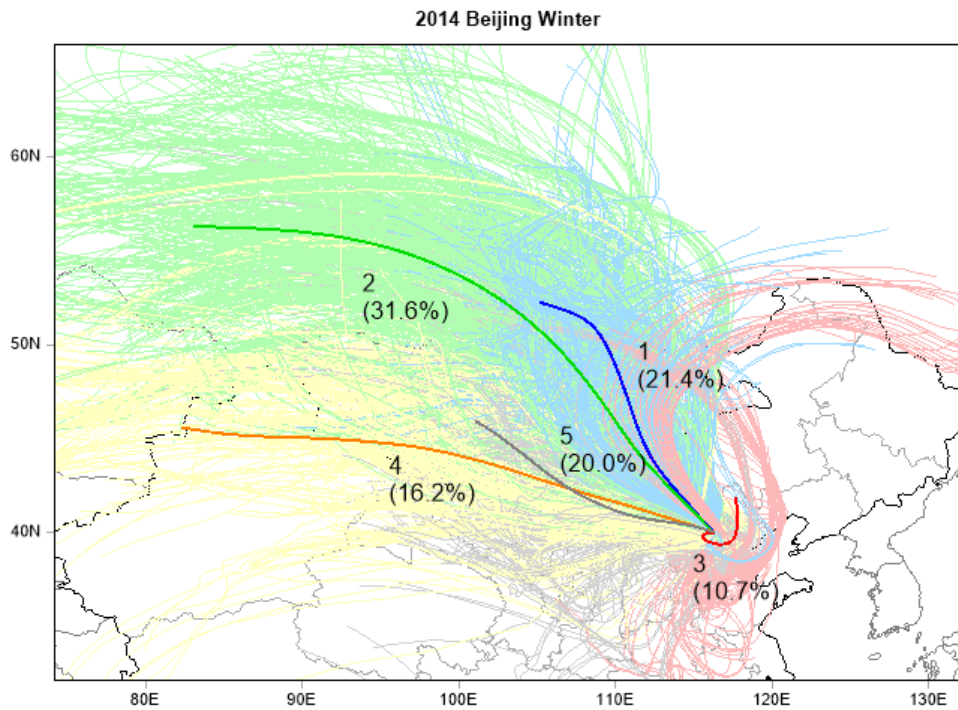




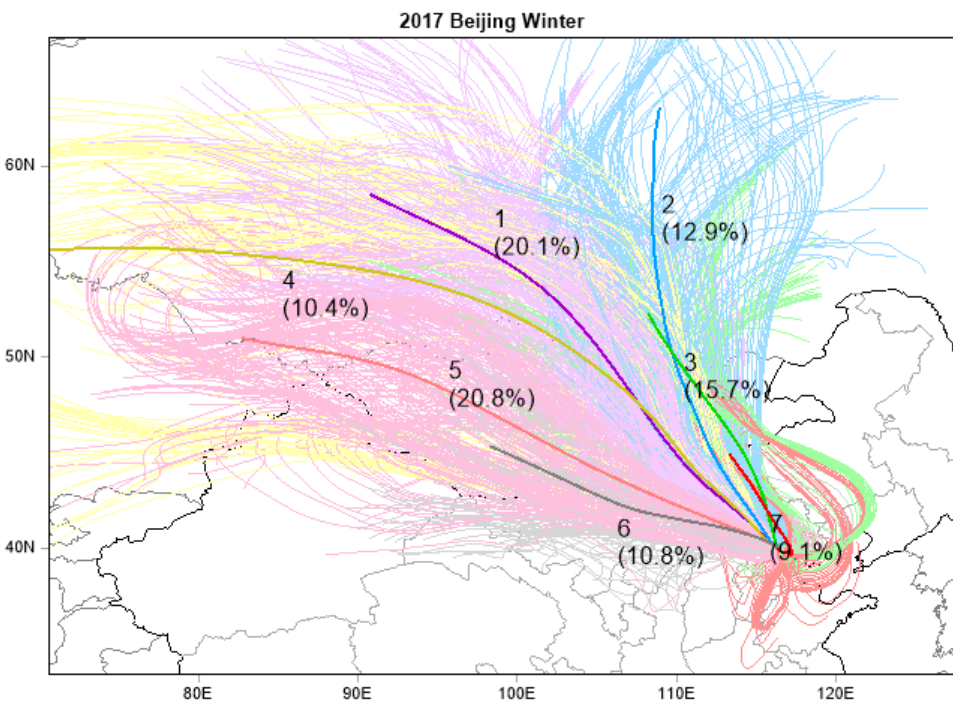
18

19 **Figure S2.** Source apportionment results of organic aerosol (OA) during the winter of 2014. (a)  
20 Mass spectra of hydrocarbon-like OA (HOA), coal combustion OA (CCOA), biomass burning OA  
21 (BBOA), and oxygenated OA (OOA). (b) Time series of different OA factors and their  
22 corresponding tracers. The correlation coefficients of OA factors with the tracers are also shown.  
23 (c) Diurnal cycles of OA factors. (d) The average fractional pie chart of OA factors to total OA.  
24 (e) The average diurnal mass contributions of OA factors to total OA.

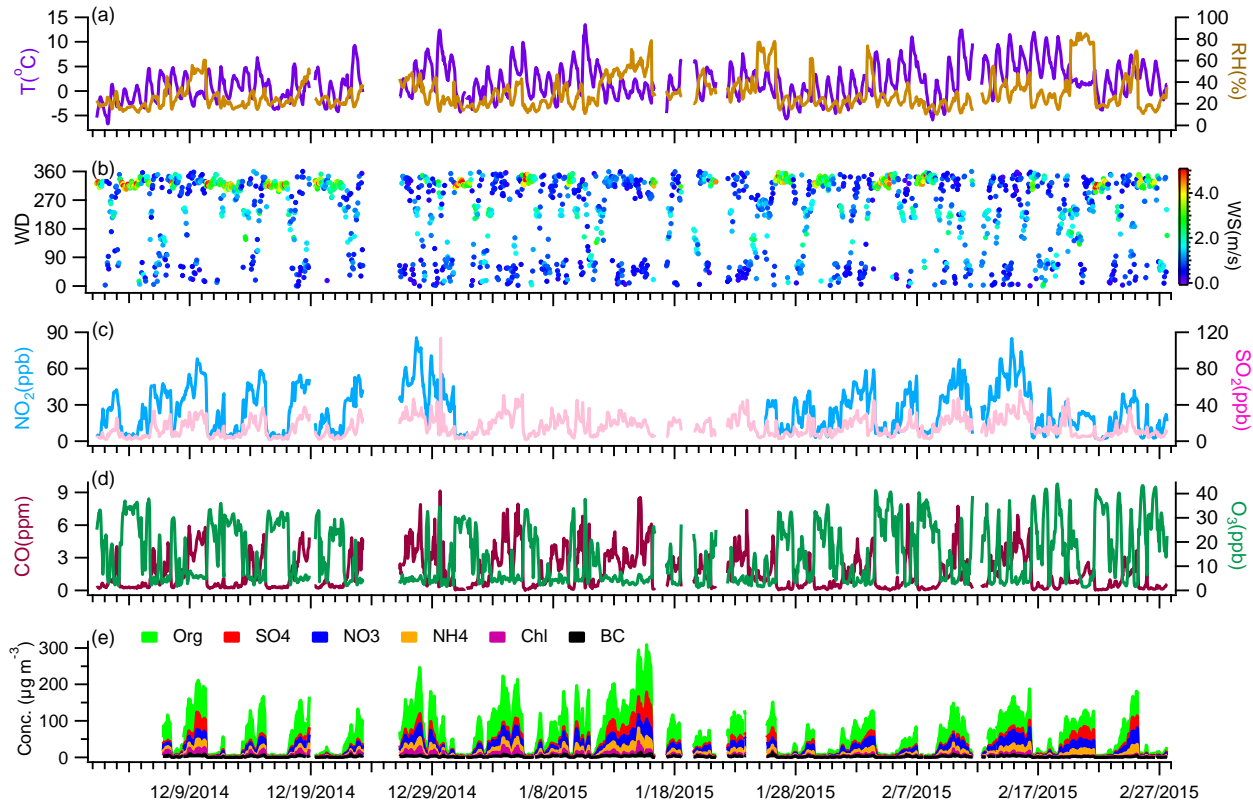
25



26

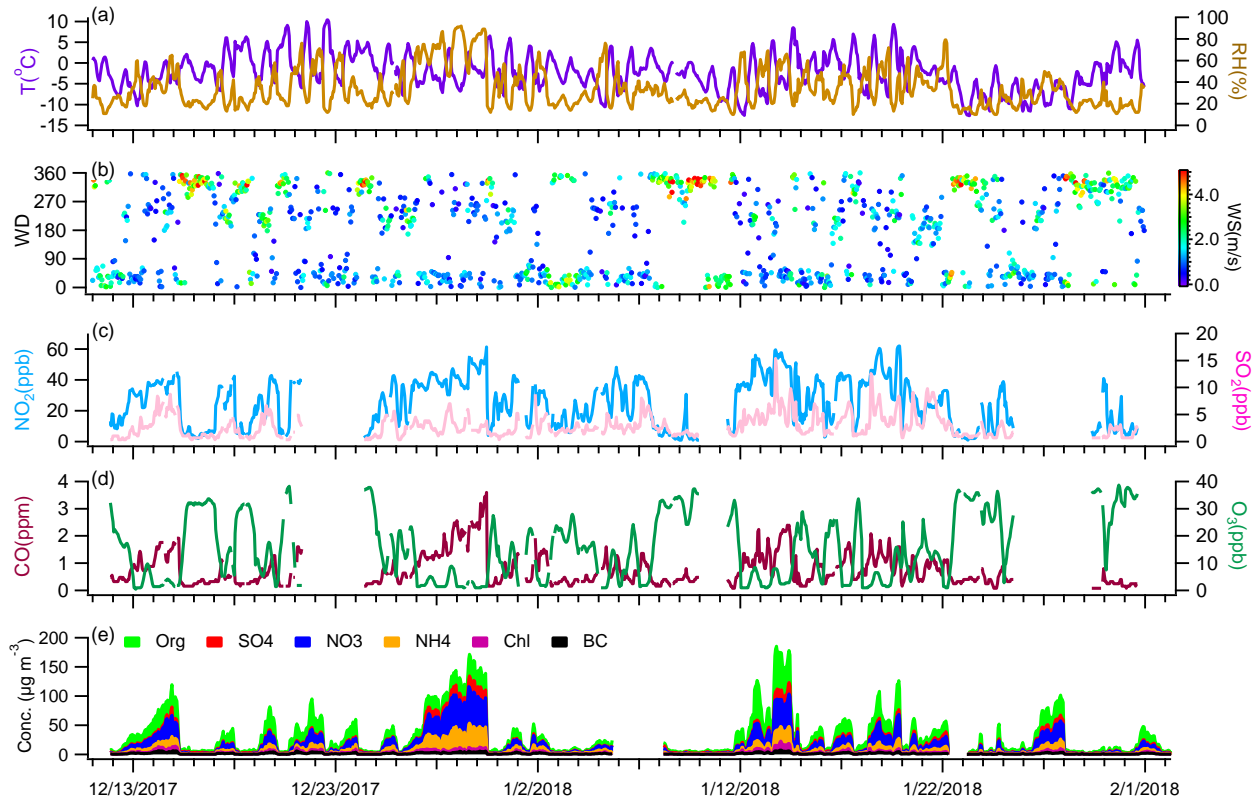
27  
28

**Figure S3.** Back trajectories of air masses arriving in Beijing in winter 2014 and winter 2017 with unique colors for different clusters. The average percentage of each cluster is shown.



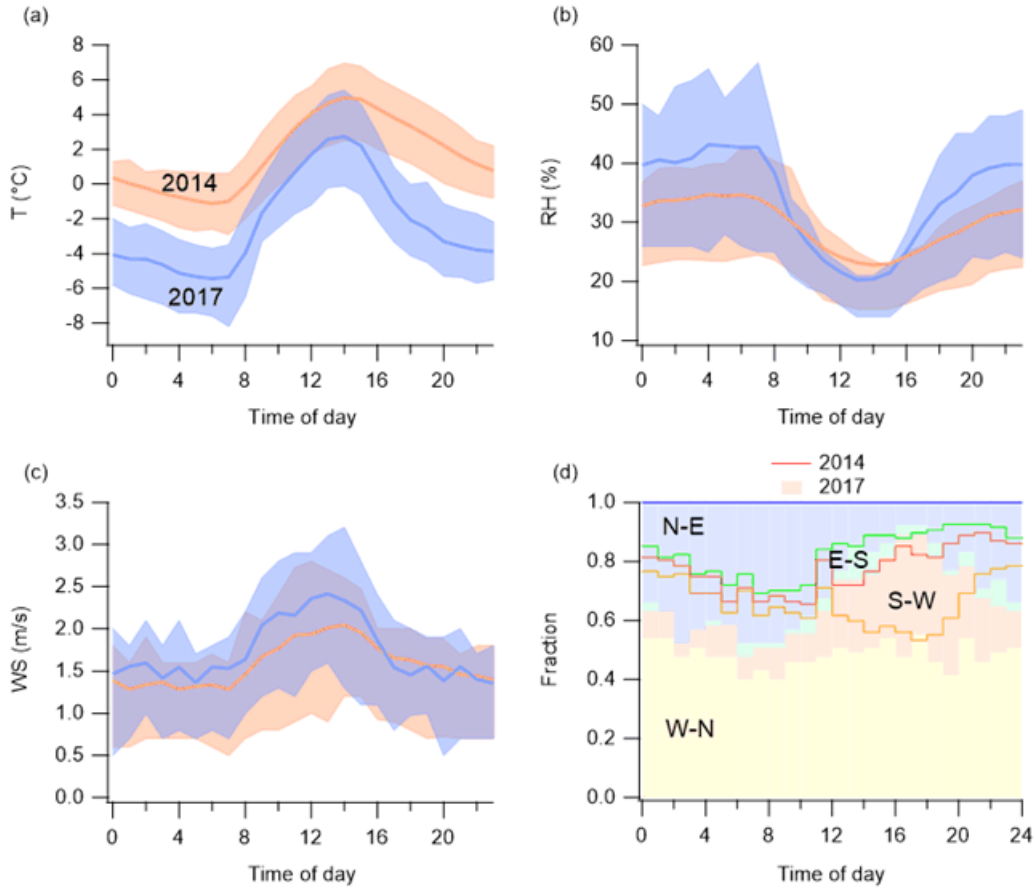
29

30 **Figure S4.** Temporal variations of (a, b) meteorological parameters, (c, d) gaseous species, and (e)  
 31 aerosol species during the winter of 2014.



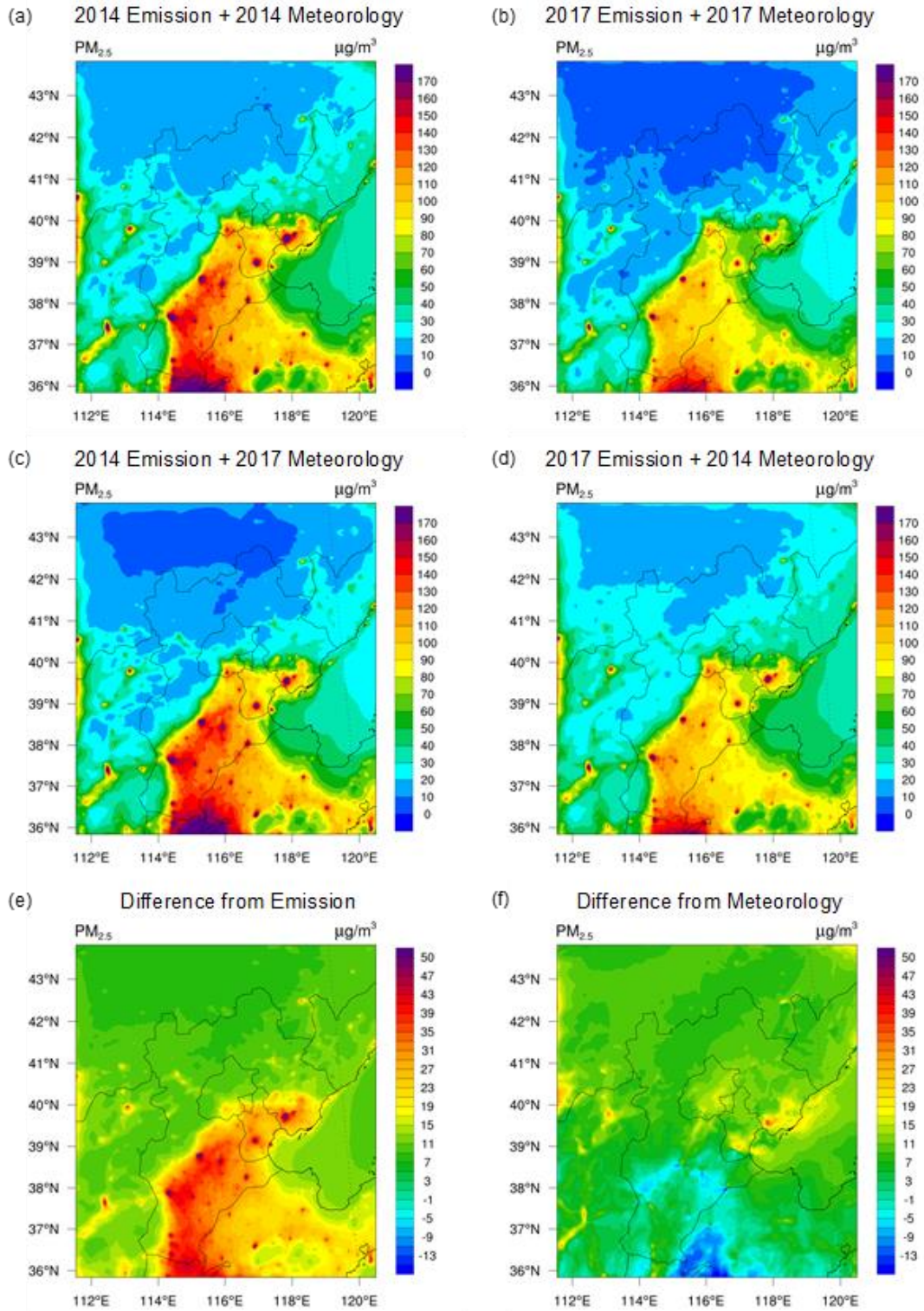
32

33 **Figure S5.** Temporal variations of (a, b) meteorological parameters, (c, d) gaseous species, and (e)  
 34 aerosol species during the winter of 2017.



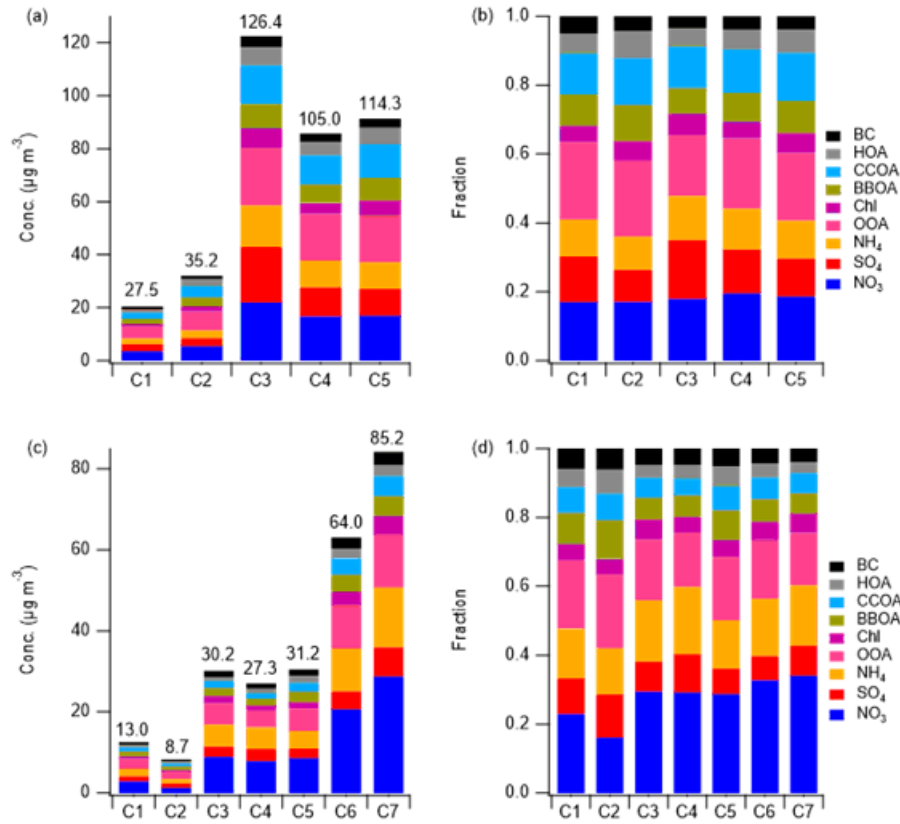
35

36 **Figure S6.** Diurnal cycles of meteorological parameters in 2014 and 2017. (a-c) The average  
 37 variations of temperature, relative humidity (RH), and wind speed (WS). The shaded areas indicate  
 38 25<sup>th</sup> and 75<sup>th</sup> percentiles. (d) The distribution of different wind directions through the day. The  
 39 lines and the stacked areas represent the year of 2014 and 2017, respectively.



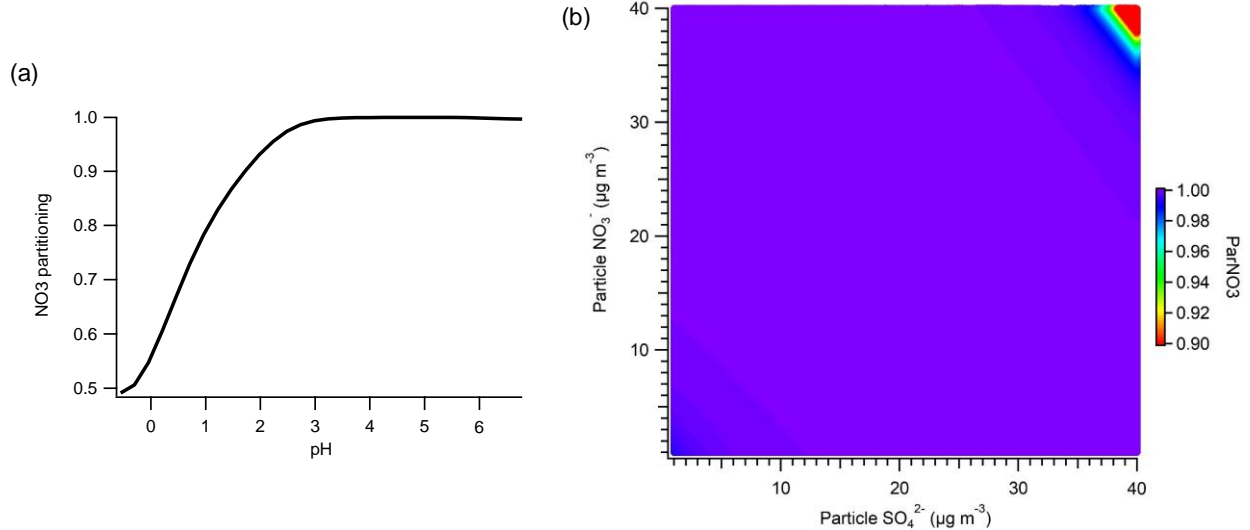
40

41 **Figure S7.** WRF-CMAQ simulated PM<sub>2.5</sub> concentration under different scenarios for the  
 42 observation periods of 2014 and 2017.



43

44 **Figure S8.** The mass concentrations of aerosol species and their fractional contributions in total  
45 PM<sub>1</sub> for different clusters in (a, b) winter 2014 and (c, d) winter 2017. The average PM<sub>1</sub>  
46 concentration of each cluster is shown on the top of the bar.



47

48 **Figure S9.** (a) Variation of  $\in (NO_3^-)$  as a function of particle pH. (b) Sensitivity of the fraction  
49 of particulate nitrate to the mass concentrations of particulate sulfate.